Can. J. Remote Sensing, Vol. 33, No. 5, pp. 431–444, 2007

Establishing the best spectral bands and timing of imagery for land use – land cover (LULC) class separability using Landsat ETM+ and Terra MODIS data

C.M. Biradar, P.S. Thenkabail, Md.A. Islam, M. Anputhas, R. Tharme, J. Vithanage, R. Alankara, and S. Gunasinghe

Abstract. The main goals of this study were to (*i*) establish Landsat enhanced thematic mapper plus (ETM+) and moderate resolution imaging spectroradiometer (MODIS) spectral bands best suited for land use – land cover (LULC) class separability, and (*ii*) study the role of the timing of imagery best suited for LULC class mapping. The study was carried out in the lower portion of the Uda Walawe River basin of southern Sri Lanka. The expansion of irrigated agriculture in this basin has resulted in several distinct changes in the LULC classes and their distribution. The area is dominated by agriculture, plantations, *chena* (slash and burn) lands with various types of natural vegetation such as degraded forests and scrubland, and wetlands with recently developed irrigation canals and tanks. The results showed that the two shortwave-infrared (SWIR) bands of Landsat ETM+ (bands centered at 1.650 and 2.220 µm) and MODIS (2.130 and 1.640 µm) and the thermal band (11.450 µm) of Landsat ETM+ were most sensitive in separating an overwhelming proportion of the 15 LULC classes studied. However, other bands, though not as powerful as thermal or SWIR bands, by themselves, often play a vital role in separating certain specific LULC classes that are not easily separable by thermal and (or) SWIR bands. The MODIS monthly time series showed that the timing of the imagery was crucial in the separability of LULC classes. An overwhelming proportion of the classes were separated from one another using the data for the two wettest months (November and December) and the driest month (July). All 15 LULC classes were separable using the three wettest months (November, December, and January) and the two driest months (June and July).

Résumé. Les objectifs principaux de cette étude étaient de : (*i*) déterminer les bandes spectrales ETM+ (« enhanced thematic mapper plus ») de Landsat et de MODIS (« moderate resolution imaging spectroradiometer ») les plus adéquates pour améliorer la séparabilité des classes d'utilisation du sol – couvert (LULC) et (*ii*) étudier le rôle du choix du moment d'acquisition des images le plus propice pour la cartographie de l'utilisation du sol – couvert. L'étude a été réalisée dans la partie inférieure du bassin du fleuve Uda Walawe, dans le sud du Sri Lanka. L'expansion de l'agriculture irriguée dans le bassin a entraîné de multiples changements visibles dans les classes de LULC et leur répartition. La zone est dominée par l'agriculture, les plantations, les terres de *chena* (agriculture sur brûlis) caractérisées par des couverts de végétation naturelle variés tels que des forêts dégradées et des savanes arbustives, et des terres humides avec des canaux et réservoirs d'irrigation développés récemment. Les résultats ont montré que les deux bandes infrarouge de courte longueur d'onde (SWIR) de ETM+ de Landsat (bandes centrées à 1,650 µm et 2,220 µm) et de MODIS (2,130 µm et 1,640 µm) de même que la bande thermique (11,450 µm) de ETM+ de Landsat étaient les plus sensibles dans la séparation de la très grande majorité des 15 classes de LULC étudiées. Toutefois, d'autres bandes, quoique moins performantes que les bandes thermiques ou SWIR, par elles-mêmes, jouent souvent un rôle primordial dans la séparation de certaines classes spécifiques de LULC qui ne sont pas facilement séparables au moyen des bandes thermiques et (ou) SWIR. Les séries chronologiques mensuelles de MODIS ont montré que le choix du moment d'acquisition de l'imagerie était crucial pour assurer la séparabilité des classes de LULC. Une très grande proportion des classes ont été séparées les unes des autres en utilisant les données des deux mois les plus humides (novembre et décembre) et le mois le plus sec (juillet). Toutes les 15 classes de LULC étaient séparables en utilisant les 3 mois les plus humides (novembre, décembre, janvier) et les deux les plus secs (juin et juillet).
[Traduit par la Rédaction]

Received 6 February 2007. Accepted 19 July 2007. Published on the *Canadian Journal of Remote Sensing* Web site at http://pubs.nrc-cnrc.gc.ca/cjrs on 7 November 2007.

C.M. Biradar.[1] International Water Management Institute, Colombo, Sri Lanka; and Institute for the Study of Earth, Oceans and Space, University of New Hampshire, Durham, NH 03824, USA.

P.S. Thenkabail, Md.A. Islam, M. Anputhas, R. Tharme, J. Vithanage, R. Alankara, and S. Gunasinghe. International Water Management Institute, Colombo, Sri Lanka.

[1]Corresponding author. (e-mail: Biradar.C.M@unh.edu).

Background and rationale

The effects of land cover conversion with significant changes can affect hydrological (Williams and Melack, 1997) and biological processes (Holscher et al., 1997). Monitoring the locations and distributions of land cover changes is important for establishing linkages between policy decisions, regulatory actions, and subsequent land-use activities (Jones et al., 1997; Biradar et al., 2004; Lunetta et al., 2006). Numerous techniques have been demonstrated for thematic change analysis using remote sensing data (Singh, 1989; Coppin and Bauer, 1996; Jensen, 1996), and these might be applicable for change detection (Singh, 1989; Stow et al., 1996) and allow the identification of major processes of change and, by inference, the characterization of land-use dynamics (Lambin and Ehrlich, 1997; Mertensl and Lambin, 1999; Biradar et al., 2003). Land cover composition and change are important factors that affect ecosystem conditions and functions. The use of satellite-based remote sensor data has been widely applied to provide a cost-effective means to develop land cover over large geographic regions (Lunetta et al., 2006).

To date, most research studies have recognized and used the entire set of bands in a sensor for land use – land cover (LULC) studies. However, there is limited information available to understand which Landsat enhanced thematic mapper plus (ETM+) spectral bands and moderate-resolution imaging spectroradiometer (MODIS) time-series months are best suited for LULC mapping, and whether there is a need to use each and every band and (or) month. Identification of optimal bands and months for mapping and characterization of LULC classes, by dropping redundant bands–months, is the most effective course of action. Also, the satellite sensor data at various time periods can never be guaranteed from any one sensor, given the availability of cloud-free images in humid tropical regions. The combination of sensor types and time series provides a better option to overcome the limitation of the data gap due to cloud cover, reduces data volumes, and provides optimal data for processing.

This research was conducted at the Uda Walawe left bank irrigation extension project in Sri Lanka. The expansion of irrigated agriculture in the Uda Walawe area has resulted in several distinct changes in the LULC classes and their distribution. An important component of the local biodiversity conservation and management was the delineation and mapping of LULC classes for preservation and restoration (Biradar et al., 2003; Garono et al., 2003). Developmental activities such as land clearing and expansion of irrigated agriculture have dramatically altered both distribution and conditions of the original LULC classes in the region. The influence of irrigated agriculture in the Uda Walawe left bank extension area can be observed almost everywhere. More than half of the landscape of Uda Walawe has been cleared for irrigated agriculture, resulting in a number of distinct LULC classes.

The primary objective of this research was to establish the best spectral bands from Landsat ETM+ and MODIS images for mapping distinct LULC classes. The secondary objective was to determine the optimum timing of MODIS data acquisition. Irrigation projects in the study area started at the end of 2001 and became operational at the end of 2003. The LULC class separability analysis and mapping were done prior to and after commissioning of the irrigation projects based on 2001 and 2003 Landsat ETM+ images. Similarly, coarse-resolution MODIS 500 m 8-day surface reflectance time series from 2002 to 2003 were used to study the optimum bands, and the same data were used to generate monthly maximum value composites (MVCs) using a time series normalized difference vegetation index (NDVI) to determine the best months for LULC class separability.

Methods

Study area

The study area lies in the lower portion of the Uda Walawe River basin of southern Sri Lanka at an elevation ranging from over 90 m to sea level on the southern coast (**Figure 1**). Precipitation varies significantly in the basin from over 3000 mm in the northern tip to around 1000 mm along the seashore. The average temperature in the area is about 28 °C (Shortt, 2001). The area is dominated by agriculture and includes plantations (banana and coconut), forestation, and chena land. Irrigation is practised in the fragmented areas through diversion of small streams in the highlands and by small tanks and reservoirs in the plains (Molle et al., 2003). The construction of the left bank irrigation system has enabled farmers to cultivate during both the main cropping season called *maha*, from October to February, and the secondary cropping season called *yala*, from April to August. The irrigated fields serve mainly for cultivation of cash crops. The main crop grown is rice, with sugarcane in fragmented patches. In the home gardens – croplands with orchards, fruits and vegetables are grown for consumption by the farmers themselves.

Data

Satellite remote sensing data

The study used coarse-resolution MODIS surface reflectance 8-day level 3 at 500 m pixel resolution images (MOD09A1, version 3) for the period 2001–2003 and medium-resolution Landsat ETM+ satellite images, whose characteristics are listed in **Table 1**. Landsat ETM+ at 30 m pixel resolution images for 14 March 2001 (before the irrigation project) and 5 April 2003 (after the irrigation project) were used for classification and spectral band separability analysis. The anomalies associated with MODIS data, such as atmospheric effects and clouds, were eliminated in the level-3 8-day composites (MOD09A1, version 3), and maximum value composites were composed for further enhancement of the time-series images by removing any traces of ambiguous pixels. In addition, 8-day and monthly MODIS time series NDVI maximum value composite (MVC) value data at 500 m resolution for the years 2001–2003 were used for time-series (phenology) analysis and spectral signature extraction to identify the best month for separating LULC class types (see processing techniques in Thenkabail et al., 2005).

Secondary and ancillary data such as topographic maps, construction maps (Nippon Koei Co. Ltd., 2005), administrative

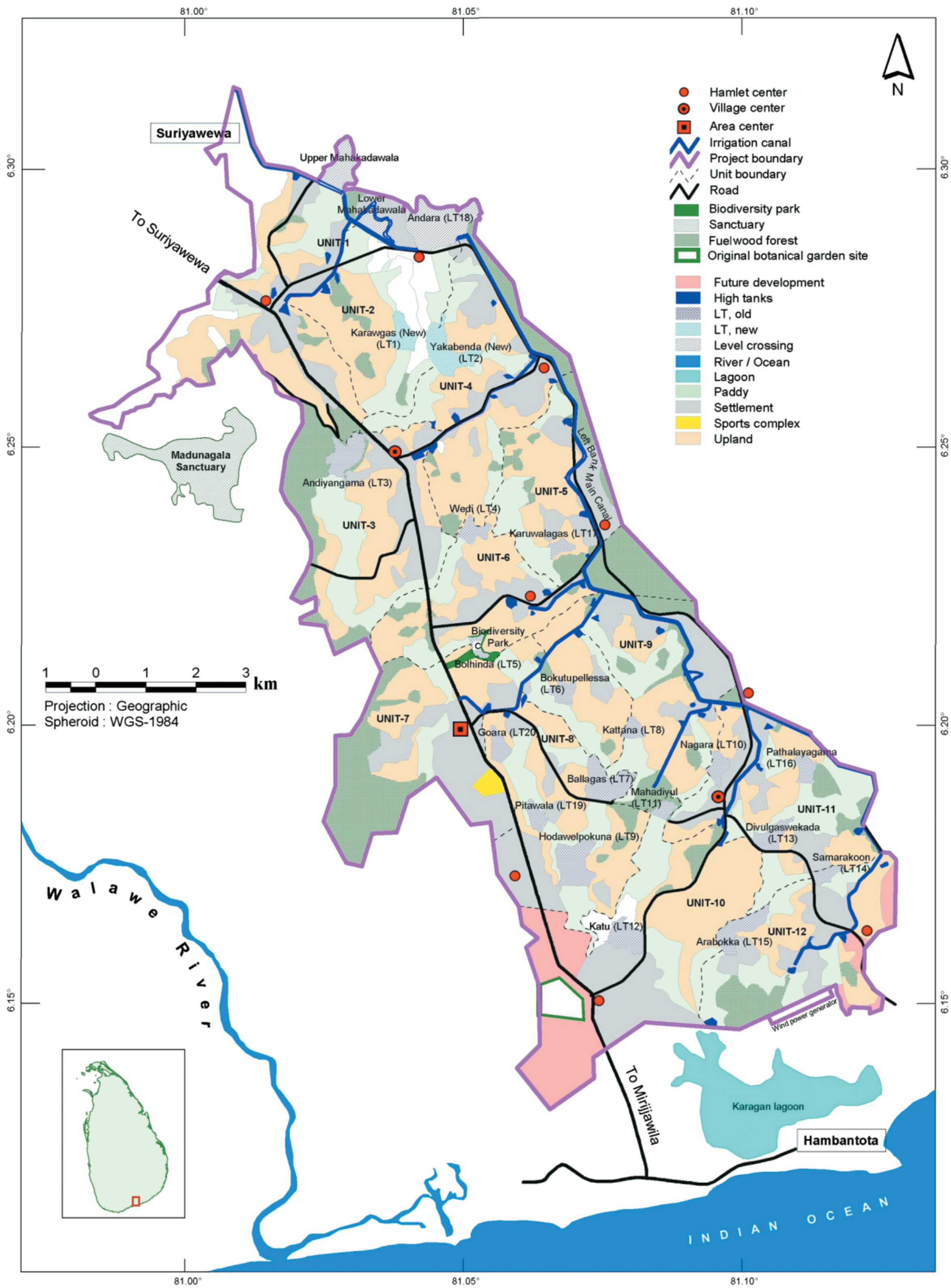

Figure 1. Location map of the study area, showing the original plan for the layout of the irrigation scheme under the Walawe left bank irrigation upgrading and extension project (source: Nippon Koei Co. Ltd., 2005).

Table 1. Characteristics of satellite sensor data used in this study.

Spatial resolution	Band used	Band number	Band range (μm)	Band center (μm)
MODIS sensor (January 2001 to December 2003)				
500 m (optical)	7	Band1	0.620–0.670	0.645
	7	Band2	0.840–0.876	0.858
	7	Band3	0.459–0.479	0.469
	7	Band4	0.545–0.565	0.555
	7	Band5	1.230–1.250	1.240
	7	Band6	1.628–1.652	1.640
	7	Band7	2.105–2.155	2.130
Landsat-7 ETM+ sensor (14 March 2001; 5 April 2003)				
30 m (optical)	6	Band1	0.450–0.515	0.483
	6	Band2	0.525–0.605	0.565
	6	Band3	0.630–0.690	0.660
	6	Band4	0.750–0.900	0.825
	6	Band5	1.550–1.750	1.650
60 m (thermal)	1	Band6	10.400–12.500	11.450
	1	Band7	2.090–2.350	2.220

boundaries, meteorological data, soil types, and agro-ecological zones from the International Water Management Institute (IWMI) Data Storehouse Pathway (International Water Management Institute, 2004) were used to aid the LULC class identification and labeling process.

Ground-truth data

Ground-truth data were collected from the field campaign from 3 to 7 May 2004. Ground-truth data from the previous field campaigns (see www.iwmidsp.org) by IWMI researchers were also used to extract information for the years 2001 and 2003. The overall sample size of ground-truth data for the 15 key LULC classes in the study area is shown in **Table 2**. During ground-truthing, information was collected on LULC class conditions, cover density for mapping, and separability analysis. The ground-truth data were organized in standard format (www.iwmidsp.org) and used in LULC class identification and labeling as per the procedures described in Thenkabail et al. (2004; 2006). Class labels were assigned in the field using a system that allows merging to a higher class or breakdown into a distinctly unique class in a hierarchical format, based on the land cover percentage taken at each location. The precise locations of the global positioning system (GPS) points referring each point detail were catalogued and linked in Arc View (Environmental Systems Research Institute, Inc., 2000) to ease information access (**Figure 2**). The data include latitude, longitude (in World Geodetic System 1984 (WGS 84) datum), altitude, LULC class, land-cover type (percentages of trees, shrubs, grasses, etc.), canopy density, irrigation system, and digital photographs at every ground-truth location. Altogether, 300 ground-truth points were collected using the stratified random sampling design. Similar classes and closely related classes, for example, scrubland–open, sparse, and dense, were grouped to reduce the number of LULC classes termed as aggregated LULC classes, whose sample sizes are shown in **Table 2**. The ground-truth data can be downloaded free of charge at the IWMI Data Storehouse Pathway (www.iwmidsp.org).

Table 2. Land use – land cover (LULC) classes and number of 90 m × 90 m ground-truth sample plots.

Class No.	Class name	No. of plots
1	Rice paddy dominant	44
2	Chena lands	28
3	Remnant degraded forest	16
4	Scrubland	38
5	Inland water bodies (deep)	16
6	Aquatic vegetation and croplands (mixed)	10
7	Home gardens – croplands with orchards	16
8	Wetlands (shallow water – marshy)	20
9	Wetlands (with aquatic vegetation)	18
10	Water body (shallow)	20
11	Fuelwood and multipurpose tree plantations	6
12	Human settlements and barren lands	20
13	Roads–canals	20
14	Bare land – fallow fields	20
15	Low herbaceous – grass cover	8

Spectral bands for class separability

The study evaluated the optimal spectral bands for class separability using Landsat ETM+ data and MODIS time series as described in the following subsections.

Landsat ETM+ spectral bands and class separability

The top-of-atmosphere reflectance values of Landsat ETM+ data for the 15 LULC classes for years 2001 (before irrigation project) and 2003 (after irrigation project) were used to test class separability. The analysis of variance, using the generalized linear model, was used to perform this exercise, and the least squared difference of means was used to distinguish the LULC

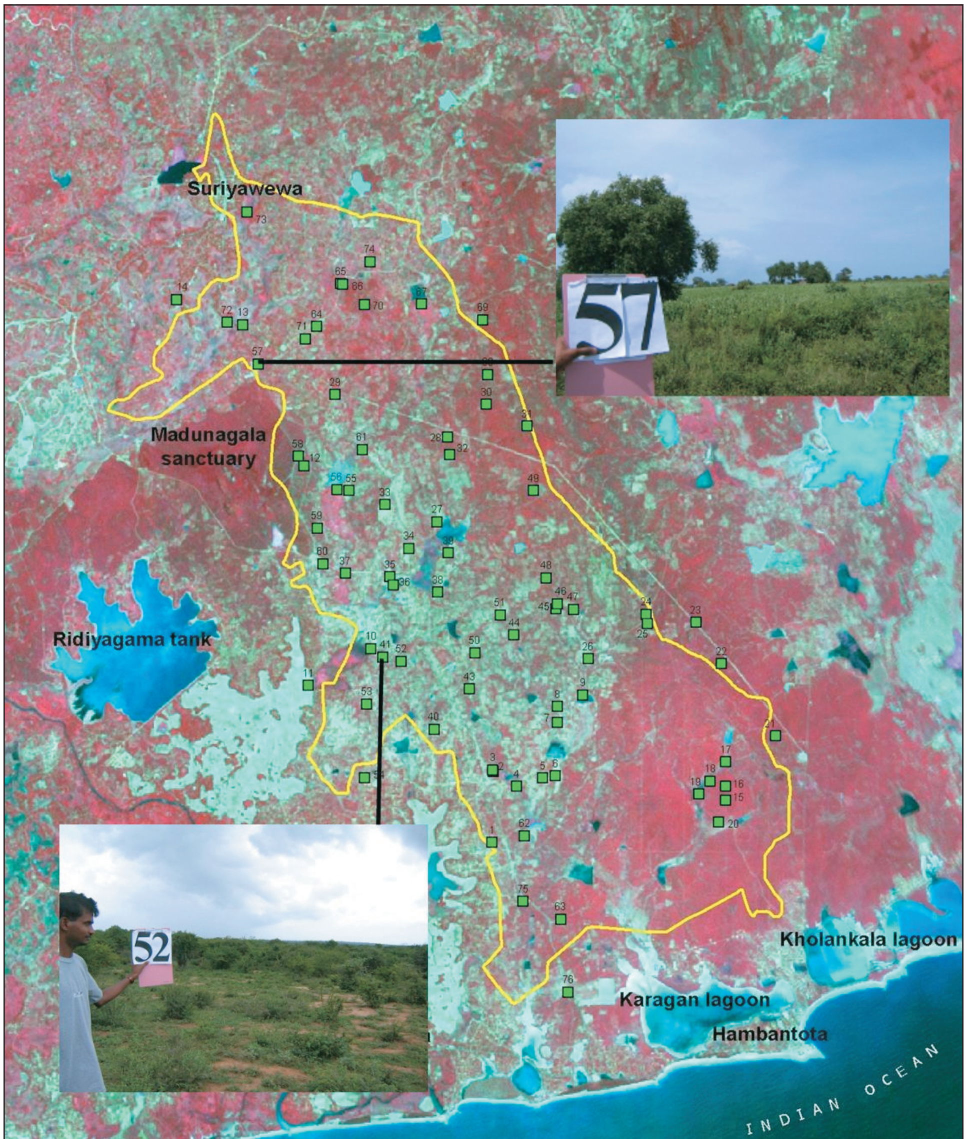

Figure 2. Locations of ground-truth sampling sites (numbered green squares) in relation to the study area (yellow border) overlaid on the Landsat ETM+ image acquired 5 April 2003. Other field information and photographs have been hyperlinked to each ground-truth point.

classes from one another. The statistical package SAS (version 9.3) was used to perform the analysis. Significant statistical differences between the LULC classes were tested at the 90% confidence level. The analysis was performed for each year (2001 and 2003) separately and for the pooled years (2001 and 2003) of the Landsat ETM+. Since the pooled data gave an output similar to that of the single-year analysis, only the pooled-data results are reported. The best bands for separating various LULC classes were identified based on the separability of LULC classes by different techniques.

MODIS time series and class separability

A analysis similar to that given in the previous section was carried out using MODIS time series. The significance of spectral differences between the LULC classes was tested at the 90% confidence level. The MODIS time-series results are discussed for each time point (monthly basis). Through this effort, the timing of the MODIS data in separating LULC classes was identified. The dominant bands associated with the best months were also identified.

LULC classification

The strategy in LULC classification was to classify and separate the 15 distinct (**Table 2**) LULC classes using class identification and labeling procedures described in Thenkabail et al. (2006; 2007) and illustrated in **Figure 3A**. The Landsat ETM+ data (**Table 1**) were classified using the iterative self-organizing data analysis technique algorithm (ISODATA) through the unsupervised classification in the ERDAS Imagine software package (Leica Geosystems, 2005).

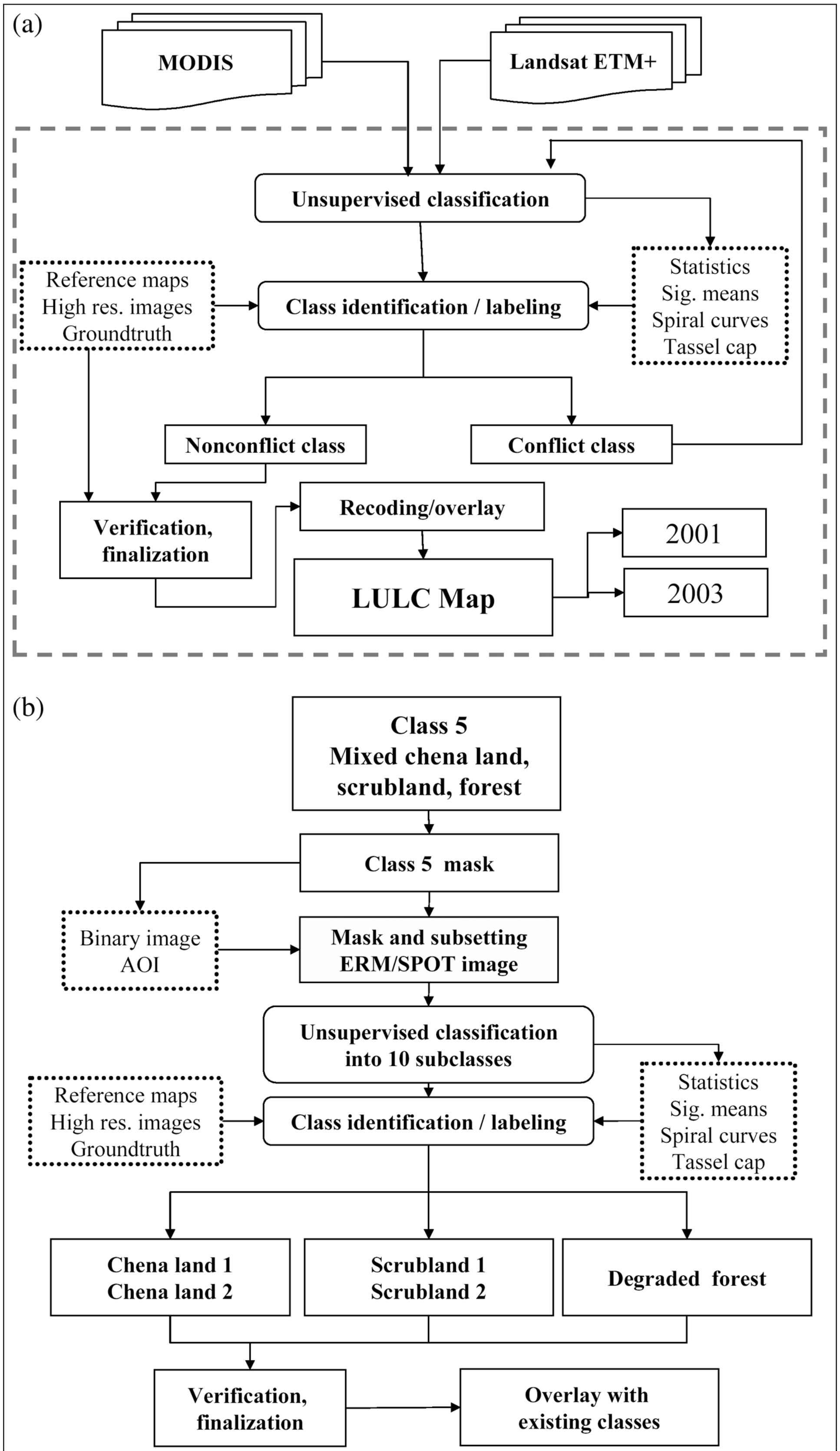

Figure 3. (A) Methodology used for mapping LULC classes. (B) Methodology used for resolving conflict (mixed) classes.

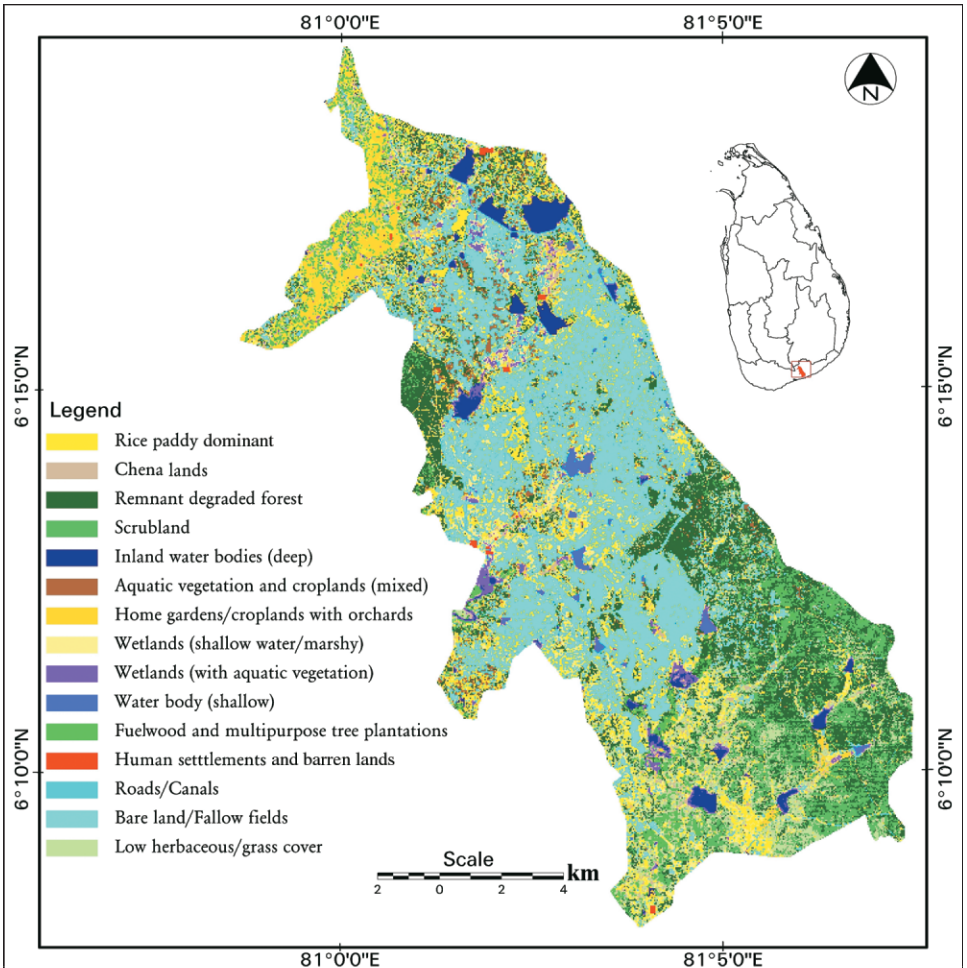

Figure 4. Land use – land cover map derived from Landsat ETM+ for the year 2003.

The spectral properties of classes were analyzed based on their distribution in brightness–greenness–wetness (BGW) tassel cap feature space and spectral curves (Thenkabail et al., 2005). Each class has been identified and labeled based on its spectral behavior in two-dimensional (2D) and three-dimensional (3D) plotting. Classes were identified and labeled based on the ground-truth information, high-resolution images, NDVI plots, and spectral curves (**Figure 3**) (Thenkabail et al., 2006). All this information was put together to perform class interpretation. Any change that occurs, even at a single pixel, was tracked by its location in brightness, greenness, and wetness feature space (Thenkabail et al., 2005). Generally, broad LULC classes were classified using the techniques explained previously.

Resolving mixed classes

Some classes were locally misclassified and intermixed with neighboring classes, and such misclassified pixels were normally identifiable using ground-truth data points where cover types were mapped out of their normal context (Fuller et al., 1998). For example, the class chena was mixed not only within scrublands as expected but also within some degraded forest areas. Such misclassifications could be removed by contextual correction methods (Groom et al., 1996; Thenkabail et al., 2006). Such pixels of mixed classes, referred to herein as conflict classes, were selectively filtered out using masking and reclassification of those selected segments (**Figure 3B**). The conflict classes were aggregated to generate a mask file that was then reclassified into 10 clusters to segregate conflict pixels, thereby identifying cropland, scrubland, and a few pixels of degraded forests (**Figure 3B**).

The segregated segment was then merged with the base map. This process of contextual correction was repeated for a number of conflict classes until all classes were properly reallocated to their likely LULC class types (Fuller et al., 1998; Thenkabail et al., 2005). Lastly, a statistical filter using a 3 × 3 kernel was run to remove unwanted salt-and-pepper effects (Schowengerdt, 1983). The main reason for this process was to remove excessive noise in the thematic map while retaining the real heterogeneity of the LULC classes (Fuller et al., 1998). The generalized, initial, disaggregated 250 subclasses were merged to produce the aggregated 15-class LULC map (**Figure 4**).

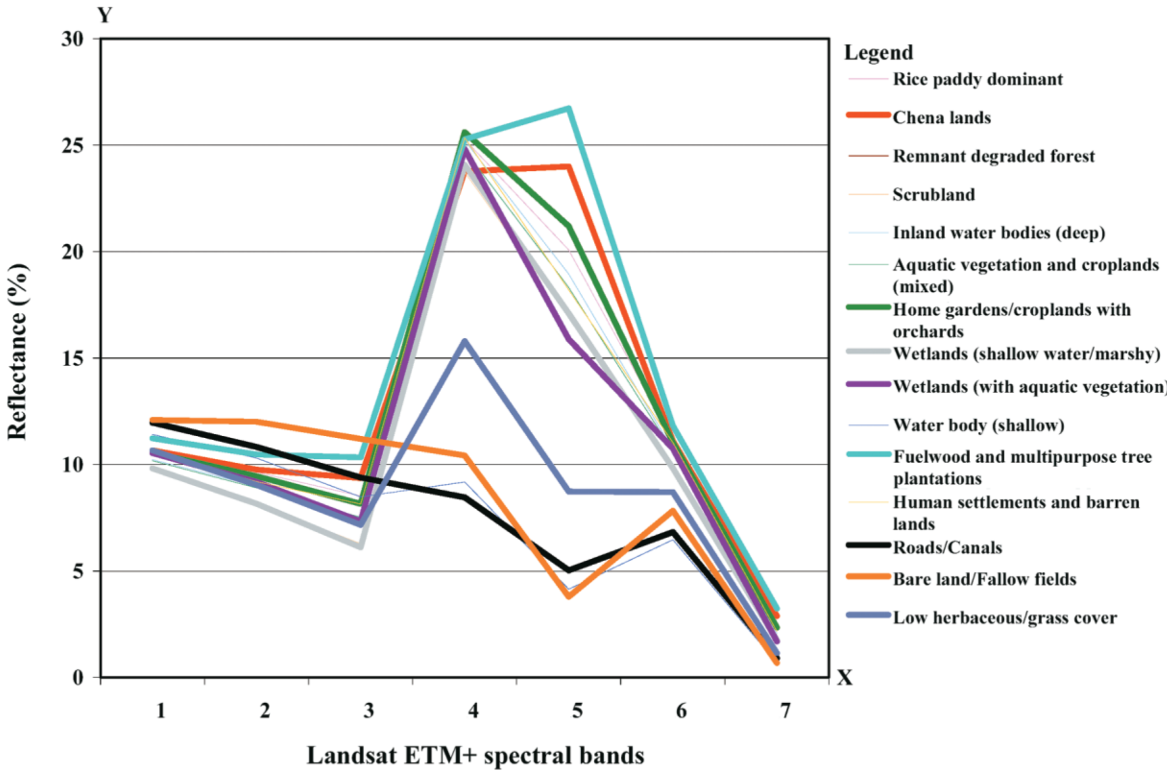

Figure 5. Spectral characteristics of the LULC classes derived from Landsat ETM+ data using ground-truth points–polygons.

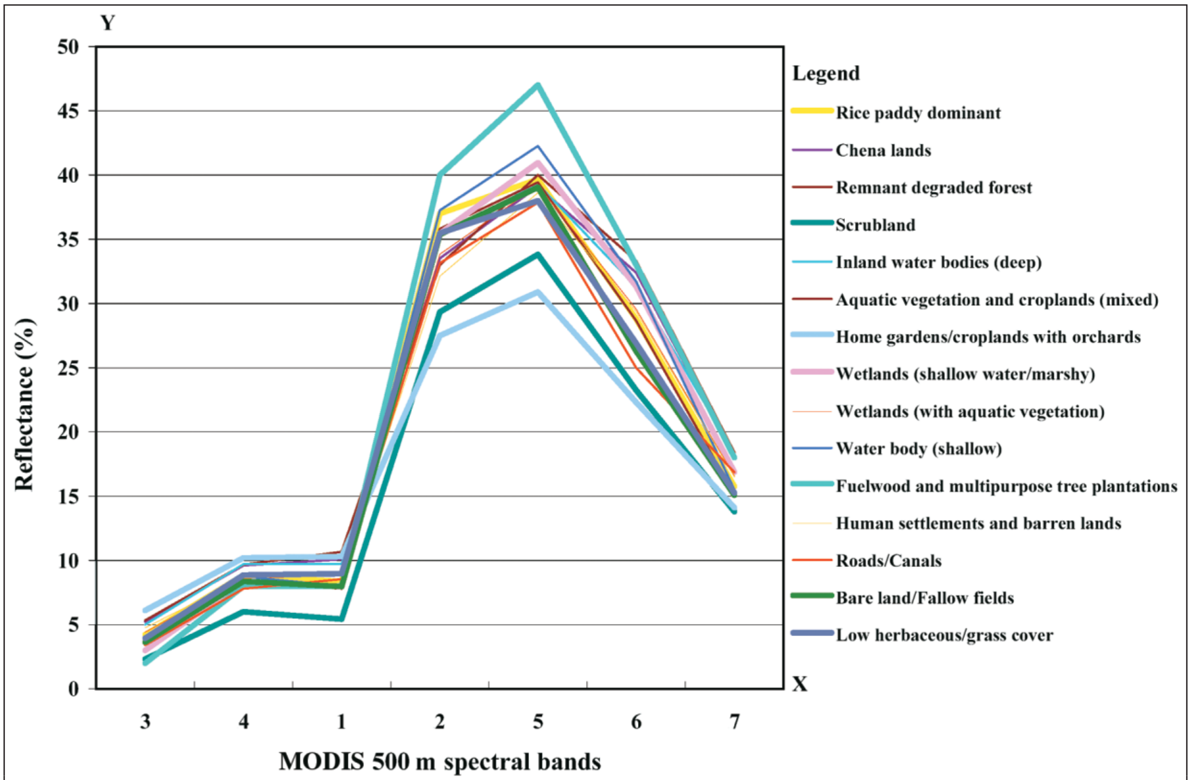

Figure 6. Spectral characteristics of the LULC classes derived using ground-truth points–polygons from MODIS 8-day surface reflectance data averaged for the months of January, November, and December 2003.

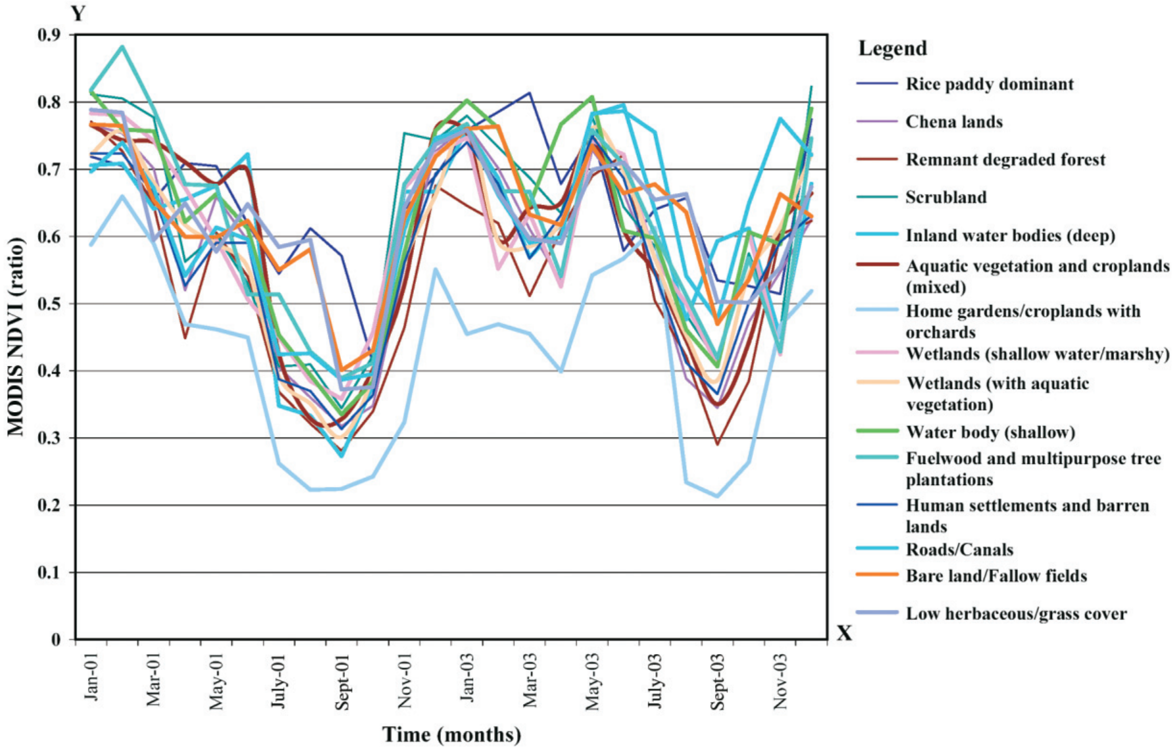

Figure 7. Spectral reflectivity of LULC classes based on MODIS monthly MVC time series NDVI data for 2001 and 2003.

Results and discussions

Spectral characteristics of the LULC classes

To develop spectral properties of the LULC classes, digital values of the satellite images were extracted from seven bands of the Landsat ETM+ data from each 3 × 3 pixel area and signature polygon identified during ground-truthing. These pixels and polygons were selected by plotting the GPS information of the sample sites on the satellite image. The mean spectral values for each LULC class for its corresponding spectral bands were plotted (**Figure 5**). Additionally, the same LULC class reflectance values also vary because of their conditions and associations. These spectral properties of the LULC classes were plotted to identify the most sensitive bands.

The mean band reflectance value of all 15 LULC classes (**Table 2**) was plotted over the spectral range of the Landsat ETM+ image (**Figure 5**). Each band shows a variable reflectance value and a corresponding curve of the LULC class properties. Healthy vegetation, such as irrigated croplands, forests, and plantations, has the highest infrared reflectance values, whereas stressed and very scattered vegetation, such as scattered scrubland, fallow lands, and water, has the lowest infrared reflectance values. The reflectivity of 15 LULC classes in various ETM+ spectral bands (**Figure 5**) is input into the SAS statistical package to assess and identify the most sensitive bands for LULC class separability. A similar procedure was used to identify the most sensitive bands (**Figure 6**) and months (**Figure 7**) in separating LULC classes based on the MODIS 500 m 8-day surface reflectance (first seven bands) (see **Table 1**) and monthly NDVI maximum value composites (MVCs) derived from the 8-day surface reflectance data.

Landsat ETM+ spectral bands separating LULC classes

The seven bands of the Landsat ETM+ data were used to evaluate the most desirable waveband for the LULC class separability, and the results are shown in **Table 3**. It was found that the human settlements and barren lands class can be separated from the rice paddy dominant class by any waveband, whereas chena lands can only be separated from the rice paddy dominant class by spectral bands 5 and 6 (**Table 3**).

The most readily separable types of LULC classes using Landsat ETM+ were (**Table 3**) bare land – fallow fields, chena lands, water body (shallow), human settlements and barren lands, inland water bodies (deep), wetlands (with aquatic vegetation), wetlands (shallow water – marshy), and wetlands (with aquatic vegetation). Fuelwood and multipurpose tree plantations was the least separable LULC class (only separable from eight other LULC classes) using Landsat ETM+ (**Table 3**). The LULC types that could not be separated from fuelwood and multipurpose tree plantations were rice paddy dominant, home gardens – croplands with orchards, remnant degraded forest, low herbaceous – grass cover, roads–canals, and scrubland (**Table 3**). Thermal data (band 6) were found to be the most desirable band in separating waterlogged rice paddy dominant from arid chena lands due to differences in surface temperature (**Table 3**), and the spectral waveband 3

Table 3. LULC class separability using pooled Landsat ETM+ data from 2001 and 2003.

	Rice paddy dominant	Bare land – fallow fields	Fuelwood and multipurpose tree plantations	Home gardens – croplands with orchards	Chena lands	Remnant degraded forest	Low herbaceous – grass cover
Rice paddy dominant	—	1, 2, 3, 5, 6, 7			5, 6	1, 2, 3, 6, 7	1, 6
Bare land – fallow fields	1, 2, 3, 5, 6, 7	—	1, 2, 3, 5, 6, 7	1, 2, 3, 5, 6	1, 2, 3, 5, 6, 7	1, 2, 3, 5, 6, 7	1, 2, 3, 5, 6, 7
Fuelwood and multipurpose tree plantations		1, 2, 3, 5, 6, 7	—		5, 6		
Home gardens – croplands with orchards		1, 2, 3, 5, 6		—	5, 6	3, 4, 6, 7	
Chena lands	5, 6	1, 2, 3, 5, 6, 7	5, 6	5, 6	—	1, 2, 3, 5, 6, 7	1, 3, 5, 6
Remnant degraded forest	1, 2, 3, 6, 7	1, 2, 3, 5, 6, 7		3, 4, 6, 7	1, 2, 3, 5, 6, 7	—	
Low herbaceous – grass cover	1, 6	1, 2, 3, 5, 6, 7			3, 4, 6, 7		—
Water body (shallow)	1, 2, 4, 5, 6, 7	3, 4, 5, 6, 7	1, 2, 4, 5, 6, 7	1, 2, 4, 5, 6, 7	1, 2, 4, 5, 6, 7	1, 2, 3, 4, 5, 6, 7	1, 2, 4, 5, 6, 7
Roads–canals		1, 2, 3, 5, 6, 7		1	5, 6	1, 2, 3, 5, 6, 7	1, 6
Scrubland	3	1, 2, 3, 5, 6, 7			3, 5, 6	2, 5, 6, 7	
Human settlements and barren lands	5	1, 2, 3, 5, 6	1	1	5, 6	1, 2, 3, 6, 7	1
Inland water bodies (deep)	1, 2, 3, 4, 5, 6, 7	1, 2, 3, 4, 5, 6, 7	1, 2, 3, 4, 5, 6, 7	1, 2, 3, 4, 5, 6, 7	1, 2, 3, 4, 5, 6, 7	1, 2, 3, 4, 5, 6, 7	1, 2, 3, 4, 5, 6, 7
Wetlands (with aquatic vegetation)	3, 4, 5, 6, 7	1, 2, 3, 4, 5, 6, 7	1, 4, 5, 6, 7	1, 4, 5, 6, 7	3, 4, 5, 6, 7	1, 4, 5, 6, 7	1, 4, 5, 6, 7
Wetlands (shallow water – marshy)	1, 2, 4, 5, 6, 7	3, 4, 5, 6, 7	1, 2, 4, 5, 6, 7	1, 2, 4, 5, 6, 7	1, 2, 4, 5, 6, 7	1, 2, 3, 4, 5, 6, 7	1, 2, 3, 4, 5, 6, 7
Aquatic vegetation and croplands (mixed)	3, 4, 5, 6, 7	1, 2, 3, 5, 6, 7	5, 6	1, 4, 5, 6, 7	3, 4, 5, 6, 7	1, 2, 5, 6	1, 5, 6
Habitat separability from all other habitats	11/14	14/14[a]	8/14[b]	10/14	14/14[a]	12/14	10/14

Note: The band numbers in each entry within the matrix denote separability between habitat classes. For example, the entry “1, 2, 3, 5, 6, 7” for bare land – fallow field versus rice paddy dominant indicate that the two classes can be separated by Landsat ETM+ bands 1, 2, 3, 5, 6, or 7.

[a]Most separable classes using Landsat ETM+ data. Bare land – fallow fields, chena lands, water body (shallow), human settlements and barren lands, inland water bodies (deep), water body (shallow), wetlands (with aquatic vegetation), and wetlands (shallow water – marshy)) can be separated from all other habitats by one or more ETM+ bands at the 90% confidence level or higher.

[b]Least separable LULC classes from Landsat ETM+ data. Fuelwood and multipurpose tree plantations can only be separated from eight other habitats (least separable) at the 10% error level.

Table 4. The MODIS NDVI MVC monthly time series in LULC class separability.

	Water body (shallow)	Human settlements and barren lands	Wetlands (shallow water – marshy)	Remnant degraded forest	Wetlands (with aquatic vegetation)	Roads–canals	Scrubland
December	14	14	14	14	13	12	10
July	13	13	12	10	10	8	10
November	14	12	13	6	12	9	7
January	14	14	7	11	4	6	5
June	14	14	12	9	11	11	8
August	14	14	13	10	13	12	7
May	14	14	14	9	9	9	9
February	14	13	14	6	12	5	9
April	14	8	7	5	5	5	7
September	14	14	12	9	12	10	8
March	13	13	10	11	10	6	7
October	13	13	10	6	7	9	8

Note: The values in the table indicate separability between habitat classes. For example, the class “water body (shallow)” was separated with significant difference from 14 other LULC classes (see **Table 3**) using MODIS data for December.

(red) was the least effective band of Landsat ETM+ in separating LULC class type. However, one cannot neglect this band to achieve the maximum separability. For instance, the LULC class rice paddy dominant can only be separated from scrubland by spectral band 3 (**Table 3; Figure 8**). When the band occurrences from **Table 3** are summarized, the study highlights the importance of shortwave infrared bands (ETM+ bands 5 and 7) and the thermal band (ETM+ band 6) as the most important bands in LULC class separability (see **Figure 8**).

Water body (shallow)	Roads–canals	Scrubland	Human settlements and barren lands	Inland water bodies (deep)	Wetlands (with aquatic vegetation)	Wetlands (shallow water – marshy)	Aquatic vegetation and croplands (mixed)
1, 2, 4, 5, 6, 7		3	5	1, 2, 3, 4, 5, 6, 7	3, 4, 5, 6, 7	1, 2, 4, 5, 6, 7	3, 4, 5, 6, 7
3, 4, 5, 6, 7	1, 2, 3, 5, 6, 7	1, 2, 3, 5, 6, 7	1, 2, 3, 5, 6	1, 2, 3, 4, 5, 6, 7	1, 2, 3, 4, 5, 6, 7	3, 4, 5, 6, 7	1, 2, 3, 5, 6, 7
1, 2, 4, 5, 6, 7			1	1, 2, 3, 4, 5, 6, 7	1, 4, 5, 6, 7	1, 2, 4, 5, 6, 7	5, 6
1, 2, 4, 5, 6, 7	1		1	1, 2, 3, 4, 5, 6, 7	1, 4, 5, 6, 7	1, 2, 4, 5, 6, 7	1, 4, 5, 6, 7
1, 2, 4, 5, 6, 7	5, 6	3, 5, 6	5, 6	1, 2, 3, 4, 5, 6, 7	3, 4, 5, 6, 7	1, 2, 4, 5, 6, 7	3, 4, 5, 6, 7
1, 2, 3, 4, 5, 6, 7	1, 2, 3, 5, 6, 7	2, 5, 6, 7	1, 2, 3, 6, 7	1, 2, 3, 4, 5, 6, 7	1, 4, 5, 6, 7	1, 2, 3, 4, 5, 6, 7	1, 2, 5, 6
1, 2, 3, 4, 5, 6, 7	1, 6		1	1, 2, 3, 4, 5, 6, 7	1, 4, 5, 6, 7	1, 2, 3, 4, 5, 6, 7	1, 5, 6
—	1, 2, 4, 5, 6, 7	1, 2, 4, 5, 6, 7	1, 2, 4, 5, 6, 7	1, 3, 4, 7	1, 2, 4, 5, 6, 7	4, 7	1, 2, 4, 5, 6, 7
1, 2, 4, 5, 6, 7	—	1		1, 2, 3, 4, 5, 6, 7	4, 5, 6, 7	1, 2, 4, 5, 6, 7	3, 5, 6
1, 2, 4, 5, 6, 7	1	—	1, 5	1, 2, 3, 4, 5, 6, 7	1, 4, 5, 6, 7	1, 2, 3, 4, 5, 6, 7	4, 5, 6
1, 2, 4, 5, 6, 7		1, 5	—	1, 2, 3, 4, 5, 6, 7	4, 5, 6, 7	1, 2, 4, 5, 6, 7	3, 4, 5, 6, 7
1, 2, 3, 4, 7	1, 2, 3, 4, 5, 6, 7	1, 2, 3, 4, 5, 6, 7	1, 2, 3, 4, 5, 6, 7	—	1, 2, 3, 4, 5, 6	1, 2, 3, 7	1, 2, 3, 4, 5, 6, 7
1, 2, 4, 5, 6, 7	4, 5, 6, 7	1, 4, 5, 6, 7	4, 5, 6, 7	1, 2, 3, 4, 5, 6	—	1, 2, 3, 4, 5, 6, 7	4, 5, 6, 7
4, 7	1, 2, 4, 5, 6, 7	1, 2, 3, 4, 5, 6, 7	1, 2, 4, 5, 6, 7	1, 2, 3, 7	1, 2, 3, 4, 5, 6, 7	—	1, 2, 3, 4, 5, 6, 7
1, 2, 4, 5, 6, 7	3, 5, 6	4, 5, 6	3, 4, 5, 6, 7	1, 2, 3, 4, 5, 6, 7	4, 5, 6, 7	1, 2, 3, 4, 5, 6, 7	—
14/14[a]	11/14	11/14	14/14[a]	14/14[a]	14/14[a]	14/14[a]	14/14[a]

Rice paddy dominant	Home gardens – croplands with orchards	Chena lands	Inland water bodies (deep)	Aquatic vegetation and croplands (mixed)	Fuelwood and multipurpose tree plantations	Bare land – fallow fields	Low herbaceous – grass cover
10	10	10	7	9	4	10	9
12	12	12	10	10	4	10	12
7	11	7	5	13	8	5	7
7	6	9	5	7	2	13	8
8	11	8	7	11	6	8	14
9	10	10	8	10	5	7	8
7	9	10	5	6	7	7	3
7	8	5	5	11	4	7	4
8	2	5	7	5	4	4	2
12	11	10	7	12	6	8	7
8	7	11	6	4	4	12	6
7	10	9	9	10	2	5	6

MODIS time series for LULC class separability

MODIS data acquisition month in LULC class separability

The MODIS monthly NDVI MVC time series were used to assess the most desirable month for LULC class separability (month giving maximum separability). The result is shown in **Table 4**. The individual LULC classes were tested with all 12 months (January–December 2001). In **Table 4**, the water body (shallow) versus the month of December intersection gives a value of 14, meaning that the water body (shallow) is

Table 5. LULC class separability using MODIS monthly time series.

	Water body (shallow)	Human settlements and barren lands	Wetlands (shallow water – marshy)	Remnant degraded forest	Wetlands (with aquatic vegetation)	Roads–canals
Water body (shallow)	—	1, 4, 7	1, 2, 4, 5	1, 2, 3, 4, 5, 6	2, 5, 6	1, 2, 4, 5, 6
Human settlements and barren lands	1, 4, 7	—	2, 5, 6	2, 3, 5, 6, 7	2, 5, 6, 7	2, 5, 6, 7,
Wetlands (shallow water – marshy)	1, 2, 4, 5	2, 5, 6	—	2, 3, 5, 6, 7	4, 5, 6	5, 6
Remnant degraded forest	1, 2, 3, 4, 5, 6	2, 3, 5, 6, 7	2, 3, 5, 6, 7	—	3, 4	3
Wetlands (with aquatic vegetation)	2, 5, 6	2, 5, 6, 7	4, 5, 6	3, 4	—	4
Roads–canals	1, 2, 4, 5, 6	2, 5, 6, 7	5,6	3	4	—
Scrubland	1, 2, 5, 6, 7	2, 5, 6, 7	2, 5, 6, 7	3	5, 6	5
Rice paddy dominant	2, 5, 6, 7	2, 5, 6, 7	1, 2, 5, 6, 7	3	7	7
Home gardens – croplands with orchards	2, 5, 6, 7	1, 2, 4, 5, 6, 7	1, 2, 4, 5, 6, 7	1, 3, 4, 7	6, 7	1, 4, 6, 7
Chena lands	2, 5, 6, 7	1, 2, 4, 5, 6, 7	1, 2, 4, 5, 6, 7	1, 3, 4, 7	6, 7	1, 4, 6, 7
Inland water bodies (deep)	2, 5, 6, 7	1, 2, 5, 6, 7	1, 2, 4, 5, 6, 7	1, 3, 4, 7	6, 7	1, 4, 6, 7
Aquatic vegetation and croplands (mixed)	1, 2, 4, 5, 6	2, 5, 6, 7	2, 5, 7	3	4	3[a]
Fuelwood and multipurpose tree plantations	2, 5, 6, 7	2, 5, 6, 7	2, 5, 6, 7	3	1, 5, 6, 7[a]	1, 3, 4[b]
Bare land – fallow fields	1, 2, 5, 6, 7	2, 5, 6, 7	2, 4, 5, 6, 7	3	5, 6	4, 5
Low herbaceous – grass cover	2, 5, 6, 7	1, 2, 5, 6, 7	1, 2, 4, 5, 6, 7	1, 3, 4, 7	5, 6, 7	1, 4, 6, 7
Habitat separability from all other habitats	14	14	14	14	14	14

Note: As in **Table 3**, the band numbers in each entry within the matrix denote separability between habitat classes using MODIS data for December and for November, May, July, January, April, and June as indicated by the footnotes.
[a]November.
[b]May.
[c]July.
[d]January.
[e]April.
[f]June.

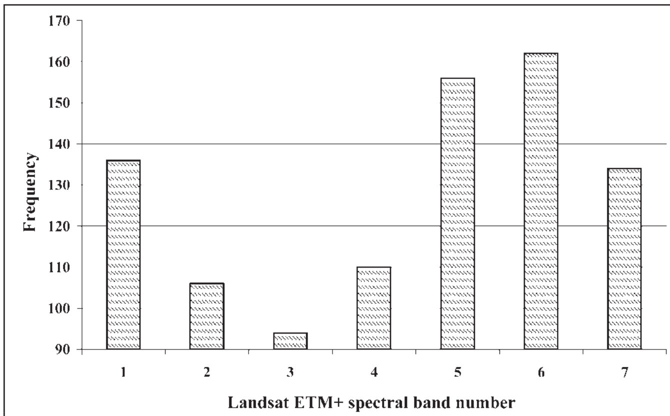

Figure 8. Most sensitive Landsat ETM+ spectral bands for LULC class separability.

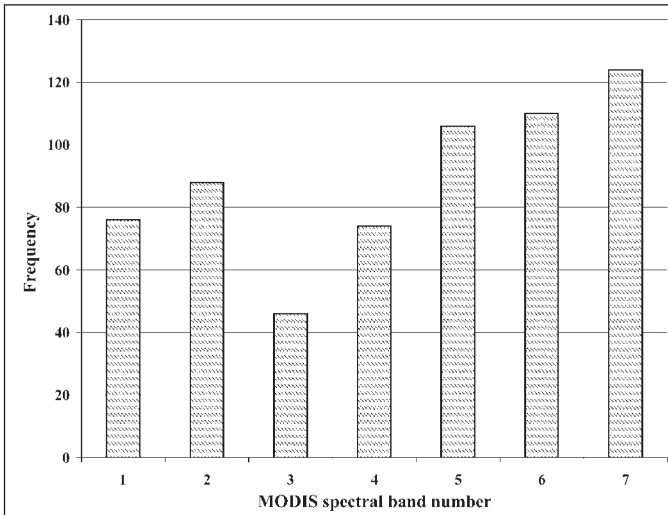

Figure 9. Most sensitive MODIS spectral bands for LULC class separability.

significantly separable from all 14 other LULC classes in the month of December. Fuelwood and multipurpose tree plantations versus December gives an intersection value of only 4, meaning that the fuelwood and multipurpose tree plantations class is significantly separable from only four other LULC classes in the month of December. Seven out of 15 LULC classes give the maximum separability in the month of December, making it the best month for LULC class separability (**Table 4**). This is followed by the month of July and then by November. These results indicate that the driest (July) and wettest (November and December) months provide the best chance of separability of LULC classes. The results indicate that separability of LULC class types is rainfall (seasonal) dependent. Further, two thirds of the LULC classes taken in this study give maximum separation from November to January, and

Scrubland	Rice paddy dominant	Home gardens – croplands with orchards	Chena lands	Inland water bodies (deep)	Aquatic vegetation and croplands (mixed)	Fuelwood and multi-purpose tree plantations	Bare land – fallow fields	Low herbaceous – grass cover
1, 2, 5, 6, 7	2, 5, 6, 7	2, 5, 6, 7	2, 5, 6, 7	2, 5, 6, 7	1, 2, 4, 5, 6	2, 5, 6, 7	1, 2, 5, 6, 7	2, 5, 6, 7
2, 5, 6, 7	2, 5, 6, 7	1, 2, 4, 5, 6, 7	1, 2, 4, 5, 6, 7	1, 2, 5, 6, 7	2, 5, 6, 7	2, 5, 6, 7	2, 5, 6, 7	1, 2, 5, 6, 7
2, 5, 6, 7	1, 2, 5, 6, 7	1, 2, 4, 5, 6, 7	1, 2, 4, 5, 6, 7	1, 2, 4, 5, 6, 7	2, 5, 7	2, 5, 6, 7	2, 4, 5, 6, 7	1, 2, 4, 5, 6, 7
3	3	1, 3, 4, 7	1, 3, 4, 7	1, 3, 4, 7	3	3	3	1, 3, 4, 7
5, 6	7	6, 7	6, 7	6, 7	4	1, 5, 6, 7[a]	5, 6	5, 6, 7
5	7	1, 4, 6, 7	1, 4, 6, 7	1, 4, 6, 7	3[a]	1, 3, 4[b]	4, 5	1, 4, 6, 7
—	5	1, 4, 7	1, 4, 7	3[c]	6, 7[c]	4[b]	3[d]	7
5	—	4	1, 4	2[c]	1, 5, 6, 7[c]	5[a]	2, 5	2, 5[c]
1, 4, 7	4	—	2, 7[c]	2[c]	1, 4, 6, 7	2[c]	1, 7	2, 3, 5[c]
1, 4, 7	1, 4	2, 7[c]	—		1, 4, 7	1, 4, 6, 7[b]	1	3, 5, 6, 7[c]
3[c]	2[c]	2[c]		—	1, 4, 6	3, 4, 7[e]	3[c]	2[d]
6, 7[c]	1, 5, 6, 7[c]	1, 4, 6, 7	1, 4, 7	1, 4, 6	—	1, 7[a]	5, 6, 7[c]	1, 4, 6, 7
4[b]	5[a]	2[c]	1, 4, 6, 7[b]	3, 4, 7[e]	1, 7[a]	—	5[a]	3[f]
3[d]	2, 5	1, 7	1	3[c]	5, 6, 7[c]	5[a]	—	7
7	2, 5[c]	2, 3, 5[c]	3, 5, 6, 7[c]	2[d]	1, 4, 6, 7	3[f]	7	—
14	14	14	13	13	14	14	14	14

one third of the LULC classes give maximum separability between June and July. The most separable LULC classes during these 5 months were water body (shallow), human settlements and barren lands, wetlands (shallow water – marshy), remnant degraded forest, and low herbaceous – grass cover; and fuelwood and multipurpose tree plantations was the least separable LULC class. Thus, maximum separability for all LULC classes can be obtained using these 5 months (**Table 4**).

MODIS spectral bands in LULC class separability

Table 5 and **Figure 9** show the results of the analysis and highlight the frequency of MODIS spectral bands in LULC class separability. Frequency refers to the number of times that particular band occurs in a 15 × 15 class matrix (out of 225). The MODIS spectral bands 1, 4, and 7 in the month of December were the most effective bands in separating the water body (shallow) class from the human settlements and barren lands class, and spectral bands 1, 5, 6, and 7 were the most sensitive in separating the fuelwood and multipurpose tree plantations class from the wetlands (with aquatic vegetation) class in the month of November (**Table 5**).

Spectral waveband 7 (centered at 2.130 µm) was the most effective MODIS band in separating the LULC class types studied, and spectral band 3 (centered at 0.469 µm) was the least effective band in separating LULC class type (see **Figure 9**). However, in some instances, such as the LULC class, the remnant degraded forest class can be separated from the roads–canals, scrubland, rice paddy dominant, wetlands (shallow water – marshy), fuelwood and multipurpose tree plantations, and bare lands – fallow fields classes using only band 3 during December (see **Table 5**).

Conclusions

This study established (*i*) the best Landsat ETM+ and MODIS spectral bands in distinguishing land use – land cover (LULC) class types, and (*ii*) the importance of timing of image acquisition in LULC class mapping.

The Landsat ETM+ thermal band 6 (band centered at 11.450 µm) closely followed by the shortwave infrared (SWIR) bands 5 (1.650 µm) and 7 (2.220 µm) were the most sensitive bands in separating the LULC class types. This was followed by the near-infrared (NIR) band 4, the green band 2, and the red band 3. The MODIS SWIR bands 7 (2.130 µm) and 6 (1.640 µm) were also the best performing bands for LULC class separability, followed by a MODIS far-NIR (FNIR) band centered at 1.240 µm and the NIR band. Overall, the results clearly demonstrated the importance of SWIR bands in LULC class studies. However, even a band such as Landsat ETM+ band 3 (red), which overall was the least sensitive band for LULC class separability, plays a crucial role in separating certain LULC classes.

There was strong evidence for the importance of the month of image acquisition in LULC class separability. The months of highest rainfall (November, December, and January) and the months of lowest rainfall (June and July) were the best periods for LULC class separability, especially the months of December (the peak rainfall month) and July (the driest month).

References

Biradar, C.M., Singh, S., and Roy, P.S. 2003. Geospatial modeling techniques for rapid assessment of biodiversity at landscape level in western Himalayas, Himachal Pradesh. *Current Science*, Vol. 84, No. 5, pp. 101–108.

Biradar, C.M., Singh, S., Das, N.K., and Roy, P.S. 2004. Wildlife–human conflict analysis in protected area: geospatial approach. In *Protected habitats*. Nature Conservators Publication. pp. 168–179.

Coppin, P.R., and Bauer, M.E. 1996. Digital change detection in forest ecosystems with remote sensing imagery. *Remote Sensing Reviews*, Vol. 13, No. 3–4, pp. 207–234.

Environmental Systems Research Institute, Inc. 2000. *ArcView 3.2 GIS and mapping software.* Environmental Systems Research Institute, Inc. (ESRI), Redlands, Calif.

Fuller, R.M., Groom, G.B., Mugisha, S., Ipulet, P., Pomeroy, D., Katende, A., Bailey, R., and Ogutu-Ohwayo, R. 1998. The integration of field survey and remote sensing for biodiversity assessment: a case study in the tropical forests and wetlands of Sango Bay, Uganda. *Biological Conservation*, Vol. 86, pp. 379–391.

Garono, R.J., Anderson, B.D., Robinson, R., and Simenstad, C. 2003. *Change in land cover along the lower Columbia River estuary as determined from LANDSAT TM imagery.* Earth Design Consult, Corvallis, Oreg. 39 pp.

Groom, G.B., Fuller, R.M., and Jones, A.R. 1996. Contextual correction: techniques for improving land cover mapping from remotely sensed images. *International Journal of Remote Sensing*, Vol. 17, pp. 69–89.

Holscher, D., Ludwig, B., Moller, R.F., and Folster, H. 1997. Dynamic of soil chemical parameters in shifting agriculture in the eastern Amazon. *Agriculture, Ecosystems & Environment*, Vol. 66, No. 2, pp. 153–163.

International Water Management Institute. 2004. *IWMI data storehouse pathway.* International Water Management Institute (IWMI), Colombo, Sri Lanka. Available from www.iwmidsp.org [cited 1 Feb. 2007].

Jensen, J.R. 1996. *Introductory digital image processing: a remote sensing perspective*. 2nd ed. Prentice-Hall Inc., Englewood Cliffs, N.J.

Jones, B.A., Ritters, K.H., Wickham, J.D., Tankersley, R.D., Jr., O'Neill, R.V., Chaloud, D.J., Smith, E.R., and Neale, A.C. 1997. *An ecological assessment of the United States mid-Atlantic region: a landscape atlas.* U.S. Environmental Protection Agency, U.S. Printing Office, Washington, D.C. Report EPA/600/R-97/130.

Lambin, E., and Ehrlich, D. 1997. Land-cover changes in sub-Saharan Africa (1982–1991): application of a change index based on remotely-sensed surface temperature and vegetation indices at a continental scale. *Remote Sensing of Environment*, Vol. 61, No. 2, pp. 181–200.

Leica Geosystems. 2005. *Earth resources data analysis system (ERDAS Imagine8.x)*. Leica Geosystems, A.G. Heinrich-Wild-Strasse, CH-9435 Heerbrugg, Switzerland.

Lunetta, R.L., Knight, F.K., Ediriwickrema, J., Lyon, J.G., and Worthy, L.D. 2006. Landcover change detection using multi-temporal MODIS NDVI data. *Remote Sensing of Environment*, Vol. 105, pp. 142–154.

Mertensl, B., and Lambin, E. 1999. Modeling land cover dynamics: integration of fine-scale land cover data with landscape attributes. *International Journal of Applied Earth Observation and Geoinformation*, Vol. 1, No. 1, pp. 48–52.

Molle, F., Jayakody, P., and de Silva, S. 2003. *Anicut systems in Sri Lanka: the case of the upper Walawe River basin.* International Water Management Institute, Colombo, Sri Lanka. Working Paper 61.

Nippon Koei Co. Ltd. 2005. *Walawe left bank irrigation upgrading and extension project. Inception report on the consultancy service*. Nippon Koei Co. Ltd., Japan, Tokyo.

Schowengerdt, R.A. 1983. *Techniques for image processing and classification in remote sensing.* Academic Press, London, UK.

Shortt, R.L. 2001. *Water quality and health: implications for irrigation management in southern Sri Lanka*. M.Eng. thesis, Department of Agricultural and Biosystems Engineering, Macdonald Campus of McGill University, Ste-Anne de Bellevue, Que.

Singh, A. 1989. Digital change detection techniques using remotely-sensed data. *International Journal of Remote Sensing*, Vol. 10, No. 6, pp. 989–1003.

Stow, D.A., Hope, A., Nguyen, A., Phinn, S.R., and Benkelman, C. 1996. Monitoring detailed land surface changes from an airborne multispectral digital camera system. *IEEE Transactions on Geosciences and Remote Sensing*, Vol. 34, No. 5, pp. 1191–1203.

Thenkabail, P.S., Enclona, E.A., Ashton, M.S., Legg, C., and De Dieu, M.J. 2004. Hyperion, IKONOS, ALI and ETM plus sensors in the study of African rainforests. *Remote Sensing of Environment*, Vol. 90, No. 1, pp. 23–43.

Thenkabail, P.S., Schull, M., and Turral, H. 2005. Ganges and Indus river basin land use/land cover (LULC) and irrigated area mapping using continuous streams of MODIS data. *Remote Sensing of Environment*, Vol. 95, No. 3, pp. 317–341.

Thenkabail, P.S., Biradar, C.M., Turral, H., Noojipady, P., Li, Y.J., Vithanage, J., Dheeravath, V., Velpuri, M., Schull, M., Cai, X.L., and Dutta, R. 2006. *An irrigated area map of the world (1999) derived from remote sensing.* International Water Management Institute, Research Report No. 105. pp. 1–74. Available from http://www.iwmigiam.org [cited 1 Feb. 2007].

Thenkabail, P.S., GangadharaRao, P., Biggs, T.W., Krishna, M., and Turral, H. 2007. Spectral matching techniques to determine historical land-use and land-cover and irrigated areas using time-series 0.1 degree AVHRR Pathfinder datasets in the Kirshna River basin, India. *Photogrammetric Engineering & Remote Sensing*, Vol. 73, No. 9, pp. 1029–1040.

Williams, M.R., and Melack, J.M. 1997. Solute export from forested and partially deforested catchments in the central Amazon. *Biogeochemistry*, Vol. 38, pp. 67–102.

